China Ocean Engineering, Vol.22, No.4, pp.533 - 546

Hill Instability Analysis of TLP Tether Subjected to Combined Platform Surge and Heave Motions*

XU Wan-hai (徐万海), ZENG Xiao-hui (曾晓辉)[1],
WU Ying-xiang (吴应湘) and LIU Jia-yue (刘家悦)
Institute of Mechanics, Chinese Academy of Sciences, Beijing 100190, China

(Received 25 September 2007; received revised form 17 September 2008; accepted 18 October 2008)

ABSTRACT

This paper presents the Hill instability analysis of Tension Leg Platform (TLP) tether in deep sea. The 2-D nonlinear beam model, which is undergoing coupled axial and transverse vibrations, is applied. The governing equations are reduced to nonlinear Hill equation by use of the Galerkin's method and the modes superposition principle. The Hill instability charted up to large parameters is obtained. An important parameter M is defined and can be expressed as the functions of tether length, the platform surge and heave motion amplitudes. Some example studies are performed for various environmental conditions. The results demonstrate that the nonlinear coupling between the axial and transverse vibrations has a significant effect on the response of structure. It needs to be considered for the accurate dynamic analysis of long TLP tether subjected to the combined platform surge and heave motions.

Key words: *Hill instability*; *parametric vibration*; *Tension Leg Platform (TLP)*; *tether*

1. Introduction

In recent years, the production and consumption of oil and other petroleum products have been rapidly increasing, which has led to the scarcity of easily retrieved oil. As a result, oil producers are motivated to go to deeper ocean to develop oil and other resources. This interest in deep water drilling has led to the in-depth study and analysis of deep water structures, such as the Tension Leg Platform (TLP) as shown in Fig. 1. The tether is one of the pivotal members of TLP, being pre-tensioned to avoid going slack due to variations in the extreme ocean environment. In the past, the dynamic behavior of slender cylindrical structure was extensively investigated (Patel and Seyed, 1995). Han and Benaroya (2000a, 2000b) studied the coupled axial and transverse vibrations of a TLP tether, derived nonlinear coupled equations of motion and obtained the free and forced responses using the finite difference approach. They proved that the nonlinear coupling became more significant with the increasing tether length. Similar equations of motion and boundary conditions were obtained by Yigit and Christoforou (1996), and the coupled vibration of the oil well drillstrings were investigated by use of the assumed mode method.

* This research was financially supported by the National High Technology Research and Development Program of China (863 Program, Grant No. 2006AA09Z350), the National Natural Science Foundation of China (Grant No. 10702073), and the Knowledge Innovation Program of Chinese Academy of Sciences (Grant No. KJCX2-YW-L02)
1 Corresponding author. E-mail: zxh@imech.ac.cn

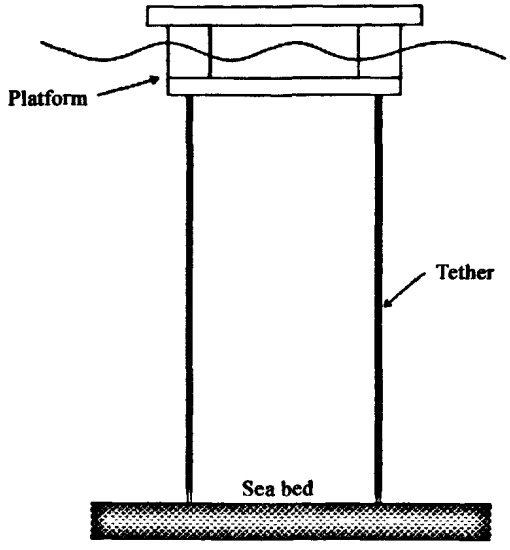

Fig. 1. Tension Leg Platform (TLP).

In general, there are mainly two directional sources of dynamic excitations exerted on the TLP tether. The first is motion induced by horizontal platform surge motion whereas the second source of dynamic excitation is due to changes in axial tension by platform heave motion. The first and second sources are respectively called a forcing excitation and a parametric excitation. Much research works has been carried out on each of these excitations applied separately to TLP tether. Jeffery and Patel (1982) extensively researched the horizontal top end forcing excitation problem. Patel and Witz (1991) introduced several kinds of forcing excitation problems of TLP tethers and risers. Hsu (1975) firstly investigated parametric excitation problem of slender marine structure. Chatjigeorgiou and Mavrakos (2002) studied the nonlinear dynamic response in the transverse direction of vertical marine risers subjected to parametric excitation at the top of the structure, the dynamic model included both elastic and bending effects, the analytical approach revealed that the dynamic lateral response was governed by effects originated from the coupling of modes in transverse direction. Chatjigeorgiou (2004) considered the dynamic behavior of vertical slender structures for marine applications under parametric excitation. The governing equations were treated by two different numerical schemes, the first was implemented by Galerkin's method and the modes superposition principle; the second method applied was a finite difference approximation scheme. Chatjigeorgiou and Mavrakos (2005) dealt with the internal resonances originated from parametric excitation of a slender pipe conveying fluid, the reported work focused on a specific case study, which corresponds to an excitation frequency equal to the double of the structure's first lateral natural frequency. Kuiper *et al.* (2007) considered the stability of a straight deep-water riser connected to a heaving floating platform. They found that a vertical harmonic motion of the platform can result in a loss of stability of the riser. Some research work has been investigated the excitations by combined platform surge and heave motions. Thampi and Niedzwecki (1992) examined the response of a non-linear marine riser to the combined excitations using Markov methods. Patel and Park (1995) investigated the combined axial and transverse response of tethers of a tensioned

buoyant platform using a semi-analytical method; the tether is modeled as a simply supported Euler-Bernoulli beam under the action of the combined axial and lateral forces. Park and Jung (2002) reported that the parametric excitation alters the response pattern of a long slender marine structure, a linear beam model was taken and a finite element method was implemented in the time domain.

In case of a harmonic parametric excitation, the amplitude of the imposed motion will define the instability regions obtained through the Mathieu equation. TLP tethers at low tensions were studied by Patel and Park (1991), and the Mathieu stability charts were derived at large parameters for TLP. It was concluded that the mean tension in the tethers could be decreased to increase the payload over the conventional design of TLP by use of the Mathieu stability charts. Wang and Zou (2006) introduced hydrodynamic aspects of in-place TLP tether design analysis with emphases on TLP hull/tether/riser coupled dynamic analysis and studied the tether Mathieu instability. Zhang *et al*. (2002) investigated TLP tether Mathieu's instability under parametric excitation. After substituting boundary conditions and including hydrodynamic damping, a beam equation (tether model) had been recast into a general Mathieu's equation. It demonstrated the importance of the damping on suppressing Mathieu's instability. Chandrasekaran *et al*. (2006) presented the dynamic analysis of tethers and TLPs considering the linearly varying tension along the tether length. The modal analysis considered a linear cable equation for tether modeling subjected to the tension varying along its length, and a Mathieu stability analysis was then performed for TLPs of different shapes and different water depth. It can be seen that increased tether tension not only leaded to a stable platform but also improved the stability due to the increased hydrodynamic load contributing to the added mass.

In case that the subject of investigation is the coupled axial and transverse vibrations of a TLP tether, the instability regions will be calculated in terms of the Hill's equation. The main aim of this paper is to obtain the Hill instability charted up to the large parameters and investigate nonlinear dynamic response of tether in different instability regions.

This paper is structured as follows. Brief description of the nonlinear structural model is given in the next section. In Section 3, the Hill instability chart is investigated by employing Hill's infinite determinant and harmonic balance method. Then, some example studies are performed in different instability regions in Section 4. Finally, conclusions are drawn based on the presented results in the last section.

2. Nonlinear Coupled Equations of Tether Vibration

The structure oscillates in both directions of the reference plane due to the externally imposed motions. Fig. 2 shows the idealized configuration under the combined excitation and gives the notation being used. For convenience the effects of torsion and rotation are neglected, the governing equations describing the coupled axial and transverse motions of TLP tether are written as follows (Han and Benaroya, 2000a, 2000b):

$$\rho A\ddot{u} - \left(EA\left(u' + \frac{1}{2}v'^2 \right) \right)' = f_x; \tag{1}$$

$$\rho A\ddot{v} - \left(EA\left(u' + \frac{1}{2}v'^2 \right) v' \right)' + (EIv'')'' = f_y. \tag{2}$$

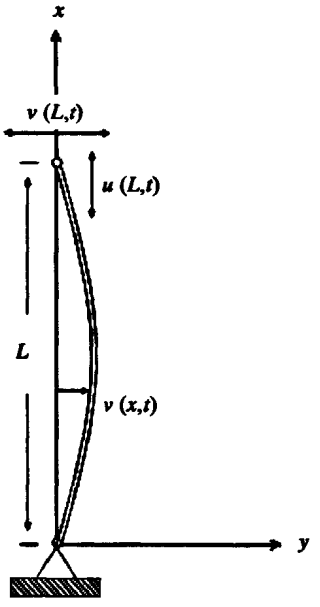

Fig. 2. Model structure configuration and notation.

It is noted that the prime notation is used for the derivative with respect to x, and dot notation with respect to t, where ρ is the tether density, A the unstretched cross-sectional area, E the modulus of elasticity, and I the unstretched moment of inertia, u is the displacement of tether in x direction and v is in y direction, f_x is the external forcing function in x direction and f_y is in y direction. With inclusion of gravity and buoyancy in the equation, f_x can be written as:

$$f_x = \rho_f A_f g - \rho A g. \tag{3}$$

The tether is considered to be completely immersed in the absence of current and waves, the transverse force is formulated by Morison's equation (Chatjigeorgiou and Mavrakos, 2002, 2005):

$$f_y = - C_A \rho_f A_f \ddot{v} - \frac{1}{2} C_D \rho_f D_0 \dot{v} \left| \dot{v} \right|. \tag{4}$$

where, D_0 is the unstretched diameter; ρ_f, the density of the surrounding fluid; g, the gravitational acceleration; A_f, the cross-section of the displaced volume; C_A, the added mass coefficient; C_D, the drag coefficient.

Assuming both ends of the structure is hinged, the motions of the lower joint and the bending moments at both ends should be equal to zero. The foregoing requirements are expressed as follows:

$$u(0,t) = 0, \quad v(0,t) = 0, \quad EIv''(0,t) = 0, \quad EIv''(L,t) = 0. \tag{5}$$

The motions at the top are assumed to be specific functions of time, thus

$$u(L,t) = u_a(t) + u_0; \tag{6}$$

$$v(L,t) = v_a(t), \tag{7}$$

where u_0 is the pre-elongation of tether due to the pre-tension provided by platform buoyancy, a consti-

tutive tension-strain relation $u_0 = N_0 L/(EA)$ has to be added, which in the present contribution is assumed to be a linear one. Note that N_0 is the pre-tension of tether, L is the original length. $u_a(t)$ and $v_a(t)$ denote the imposed external excitations in the axial and transverse direction at the tether upper end. The initial position of the top end is set to be at the midpoint of the surge motion and in the highest position of heave motion. In addition, the top end rotates in the clockwise direction by the wave-induced surface platform motion. Therefore, $u_a(t)$ and $v_a(t)$ can be written as:

$$u_a(t) = U_a \cos\omega t, \tag{8}$$

$$v_a(t) = V_a \sin\omega t, \tag{9}$$

where U_a is the platform heave motion amplitude, V_a is the platform surge motion amplitude, and ω is the angular frequency of the top end motion, which is the same as wave frequency.

The partial differential Eqs. (1) and (2) are reduced to ordinary nonlinear differential equations by applying the Galerkin's method and the modes superposition principle (Chatjigeorgiou, 2004); the solution of unknowns u and v can be expressed by:

$$u(x,t) = u_a(t)\frac{x}{L} + \frac{xN_0}{EA} + \sum_1^n u_n(t)\sin\frac{n\pi x}{L}; \tag{10}$$

$$v(x,t) = v_a(t)\frac{x}{L} + \sum_1^n v_n(t)\sin\frac{n\pi x}{L}, \tag{11}$$

where $u_n(t)$ is the amplitude of n-th order in axial direction and $v_n(t)$ is in transverse direction.

Introducing $u(x,t)$ and $v(x,t)$ from Eqs. (10) and (11) into the system of Eqs. (1) and (2) and utilizing the orthogonality relation of modes, multiplying throughout by $\sin(n\pi x/L)$ and integrating over the length of the tether, the governing equations are transformed into an infinite set of nonlinear differential equations with respect to the time dependent generalized variables $u_n(t)$ and $v_n(t)$.

$$\begin{aligned}&\ddot{u}_n(t) + \frac{EA}{\rho A}\left(\frac{n\pi}{L}\right)^2 u_n(t) + \frac{EA}{\rho A}\left(\frac{n\pi}{L}\right)^2 \frac{v_a(t)}{L} v_n(t) + (-1)^{n+1}\frac{2}{n\pi}\ddot{v}_a(t)\\ &= \left[1-(-1)^n\right]\frac{2}{\rho A n\pi}(\rho_f A_f g - \rho A g);\end{aligned} \tag{12}$$

$$\begin{aligned}&\ddot{v}_n(t) + \frac{EI\left(\frac{n\pi}{L}\right)^4 + EA\left(\frac{u_a(t)}{L} + \frac{N_0}{EA}\right)\left(\frac{n\pi}{L}\right)^2 + \frac{3}{2}EA\left(\frac{n\pi}{L}\right)^2\left(\frac{v_a(t)}{L}\right)^2}{\rho A + C_A\rho_f A_f} v_n(t)\\ &+ \frac{EA\left(\frac{n\pi}{L}\right)^2\frac{v_a(t)}{L}}{\rho A + C_A\rho_f A_f} u_n(t) + (-1)^{n+1}\frac{2}{n\pi}\ddot{v}_a(t)\\ &= -\frac{C_D\rho_f D_0}{L(\rho A + C_A\rho_f A_f)}\int_0^L Q|Q|\sin\frac{n\pi x}{L}\mathrm{d}x,\end{aligned} \tag{13}$$

where

$$Q = \dot{v}_a(t)\frac{x}{L} + \sum_1^n \dot{v}_n(t)\sin\frac{n\pi x}{L}. \tag{14}$$

Since the internal resonances which involve the elastic eigenfrequencies obtain extremely high values because the flexural rigidity EA is considerably higher than the bending stiffness EI, it is safe to

ignore the axial vibration, and the investigation will be restricted to the transverse motion only (Chatjigeorgiou and Mavrakos, 2002). It is convenient to introduce a dimensionless time variable, τ, such that:

$$2\tau = \omega t, \text{ then } \frac{d^2 v_n}{dt^2} = \frac{\omega^2}{4}\frac{d^2 v_n}{d\tau^2}. \tag{15}$$

Substituting Eq. (15) into Eq. (13) gives the final equation:

$$\frac{d^2 v_n}{d\tau^2} + \left[\delta + \varepsilon r(\tau)\right] v_n + c\int_0^L Q\left|Q\right|\sin\frac{n\pi x}{L}dx = (-1)^n \frac{\omega}{n\pi}\ddot{v}_a(\tau), \tag{16}$$

where

$$\delta = \frac{4}{\omega^2}\frac{EI(\frac{n\pi}{L})^4 + N_0(\frac{n\pi}{L})^2 + \frac{3}{4}EA(\frac{n\pi}{L})^2(\frac{V_a}{L})^2}{\rho A + C_A\rho_f A_f}; \tag{17}$$

$$c = \frac{C_D\rho_f D_0}{L(\rho A + C_A\rho_f A_f)}; \tag{18}$$

$$r(\tau) = \cos(2\tau) - M\cos(4\tau); \tag{19}$$

$$M = \frac{3}{4}\frac{V_a^2}{LU_a}. \tag{20}$$

Assuming $N^* = EAU_a/L$, N^* being the time-varying axial force amplitude, then

$$\varepsilon = \frac{4EA(\frac{n\pi}{L})^2 U_a}{\omega^2 L(\rho A + C_A\rho_f A_f)} = \frac{4(\frac{n\pi}{L})^2 N^*}{\omega^2(\rho A + C_A\rho_f A_f)}. \tag{21}$$

Eq. (16) is the nonlinear Hill equation. It is shown that, in case of a harmonic parametric excitation, or combined forcing and parametric excitation with linear beam model, $M = 0$. Then the nonlinear Hill equation becomes Mathieu equation, which can be written as:

$$\frac{d^2 v_n}{d\tau^2} + (\delta^* + \varepsilon\cos 2\tau)v_n + c\int_0^L Q\left|Q\right|\sin\frac{n\pi x}{L}dx = (-1)^n\frac{\omega}{n\pi}\ddot{v}_a(\tau) \tag{22}$$

where

$$\delta^* = \frac{4}{\omega^2}\frac{EI(\frac{n\pi}{L})^4 + N_0(\frac{n\pi}{L})^2}{\rho A + C_A\rho_f A_f}. \tag{23}$$

3. Instability Charts of Hill Equation

In actual conditions in deep sea, δ and ε may be not small parameters, therefore, the perturbation method can not be adopted. In this paper, the Hill instability chart is gained by use of the Hill's infinite determinant and harmonic balance method (Koo, 2003; Simakhina, 2003). The canonical form of the Hill equations takes its form by excluding the nonlinear damping term of Eq. (16):

$$\frac{d^2 v_n}{d\tau^2} + \left[\delta + \varepsilon r(\tau)\right] v_n = 0. \tag{24}$$

It is known that when δ in Eq. (24) belongs to a certain countable set of characteristic values,

Eq. (24) is satisfied by one of the following periodic solutions (Patel and Park, 1991):

$$v_n(\tau) = \sum_{n=0}^{\infty} a_{2n}\cos 2n\tau \qquad \text{(Even solution of period } \pi) \tag{25}$$

$$v_n(\tau) = \sum_{n=0}^{\infty} a_{2n+1}\cos(2n+1)\tau \qquad \text{(Even solution of period } 2\pi) \tag{26}$$

$$v_n(\tau) = \sum_{n=0}^{\infty} b_{2n}\sin 2n\tau \qquad \text{(Odd solution of period } \pi) \tag{27}$$

$$v_n(\tau) = \sum_{n=0}^{\infty} b_{2n+1}\sin(2n+1)\tau \qquad \text{(Odd solution of period } 2\pi) \tag{28}$$

Substituting Eqs. (25) ~ (28) into Eq. (24) and the coefficients of $\cos(2n\tau)$, $\cos(2n+1)\tau$, $\sin(2n\tau)$, $\sin(2n+1)\tau$ are equaled to zero for $n = 0, 1, 2\cdots$, then recurrence relations are obtained. With some manipulation, these recurrence relations can be expressed into infinite and terminated continued fractions.

$$\begin{vmatrix}
\delta & \frac{\varepsilon}{2} & -\frac{\varepsilon M}{2} & 0 & 0 & \cdots & 0 \\
\varepsilon & \delta-4 & \frac{\varepsilon}{2} & -\frac{\varepsilon M}{2} & 0 & \cdots & 0 \\
-\frac{\varepsilon M}{2} & \frac{\varepsilon}{2} & \delta-16 & \frac{\varepsilon}{2} & -\frac{\varepsilon M}{2} & \cdots & \cdots \\
\cdots & \cdots & \cdots & \cdots & \cdots & \cdots & \cdots \\
\cdots & \cdots & -\frac{\varepsilon M}{2} & \frac{\varepsilon}{2} & \delta-4(n-2)^2 & \frac{\varepsilon}{2} & -\frac{\varepsilon M}{2} \\
0 & \cdots & \cdots & -\frac{\varepsilon M}{2} & \frac{\varepsilon}{2} & \delta-4(n-1)^2 & \frac{\varepsilon}{2} \\
0 & 0 & 0 & \cdots & -\frac{\varepsilon M}{2} & \frac{\varepsilon}{2} & \delta-4n^2
\end{vmatrix} = 0 \tag{29}$$

$$\begin{vmatrix}
\varepsilon-4+\frac{\varepsilon M}{2} & \frac{\varepsilon}{2} & -\frac{\varepsilon M}{2} & 0 & 0 & \cdots & 0 \\
\frac{\varepsilon}{2} & \delta-16 & \frac{\varepsilon}{2} & -\frac{\varepsilon M}{2} & 0 & \cdots & 0 \\
-\frac{\varepsilon M}{2} & \frac{\varepsilon}{2} & \delta-36 & \frac{\varepsilon}{2} & -\frac{\varepsilon M}{2} & \cdots & \cdots \\
\cdots & \cdots & \cdots & \cdots & \cdots & \cdots & \cdots \\
\cdots & \cdots & -\frac{\varepsilon M}{2} & \frac{\varepsilon}{2} & \delta-4(n-2)^2 & \frac{\varepsilon}{2} & -\frac{\varepsilon M}{2} \\
0 & \cdots & \cdots & -\frac{\varepsilon M}{2} & \frac{\varepsilon}{2} & \delta-4(n-1)^2 & \frac{\varepsilon}{2} \\
0 & 0 & 0 & \cdots & -\frac{\varepsilon M}{2} & \frac{\varepsilon}{2} & \delta-4n^2
\end{vmatrix} = 0 \tag{30}$$

$$\begin{vmatrix} \delta-1+\frac{\varepsilon}{2} & \frac{\varepsilon}{2}-\frac{\varepsilon M}{2} & -\frac{\varepsilon M}{2} & 0 & 0 & \cdots & 0 \\ \frac{\varepsilon}{2}-\frac{\varepsilon M}{2} & \delta-9 & \frac{\varepsilon}{2} & -\frac{\varepsilon M}{2} & 0 & \cdots & 0 \\ -\frac{\varepsilon M}{2} & \frac{\varepsilon}{2} & \delta-25 & \frac{\varepsilon}{2} & -\frac{\varepsilon M}{2} & \cdots & \cdots \\ \cdots & \cdots & \cdots & \cdots & \cdots & \cdots & \cdots \\ \cdots & \cdots & -\frac{\varepsilon M}{2} & \frac{\varepsilon}{2} & \delta-(2n-5)^2 & \frac{\varepsilon}{2} & -\frac{\varepsilon M}{2} \\ 0 & \cdots & \cdots & -\frac{\varepsilon M}{2} & \frac{\varepsilon}{2} & \delta-(2n-3)^2 & \frac{\varepsilon}{2} \\ 0 & 0 & 0 & \cdots & -\frac{\varepsilon M}{2} & \frac{\varepsilon}{2} & \delta-(2n-1)^2 \end{vmatrix} = 0 \quad (31)$$

$$\begin{vmatrix} \delta-1-\frac{\varepsilon}{2} & \frac{\varepsilon}{2}+\frac{\varepsilon M}{2} & -\frac{\varepsilon M}{2} & 0 & 0 & \cdots & 0 \\ \frac{\varepsilon}{2}+\frac{\varepsilon M}{2} & \delta-9 & \frac{\varepsilon}{2} & -\frac{\varepsilon M}{2} & 0 & \cdots & 0 \\ -\frac{\varepsilon M}{2} & \frac{\varepsilon}{2} & \delta-25 & \frac{\varepsilon}{2} & -\frac{\varepsilon M}{2} & \cdots & \cdots \\ \cdots & \cdots & \cdots & \cdots & \cdots & \cdots & \cdots \\ \cdots & \cdots & -\frac{\varepsilon M}{2} & \frac{\varepsilon}{2} & \delta-(2n-5)^2 & \frac{\varepsilon}{2} & -\frac{\varepsilon M}{2} \\ 0 & \cdots & \cdots & -\frac{\varepsilon M}{2} & \frac{\varepsilon}{2} & \delta-(2n-3)^2 & \frac{\varepsilon}{2} \\ 0 & 0 & 0 & \cdots & -\frac{\varepsilon M}{2} & \frac{\varepsilon}{2} & \delta-(2n-1)^2 \end{vmatrix} = 0 \quad (32)$$

The first important result obtained from the conducted analysis is the Hill instability regions for the coupled axial and transverse vibration of a TLP tether. Only a finite number of terms in Eqs. (25) ~ (28) is taken, and n is set to be 10. Fig. 3 demonstrates the first five instability regions obtained through Eq. (24) with $M = 0$, $M = 0.1085$, and $M = 0.3014$, for the tether properties listed in Table 1.

Table 1 Values of the system parameters used in calculations (Patel and Park, 1995)

Length (m)	300	Outer diameter (m)	0.812
Dry mass (kg/m^3)	726.3	Added mass coefficient	1.0
Flexural rigidity (Nm^2)	14.57×10^8	Axial rigidity (N)	1.88×10^{10}
Inner diameter (m)	0.762	Drag coefficient	0.8
Surge amplitude (m)	3.0	Top tension (N)	13.0×10^6

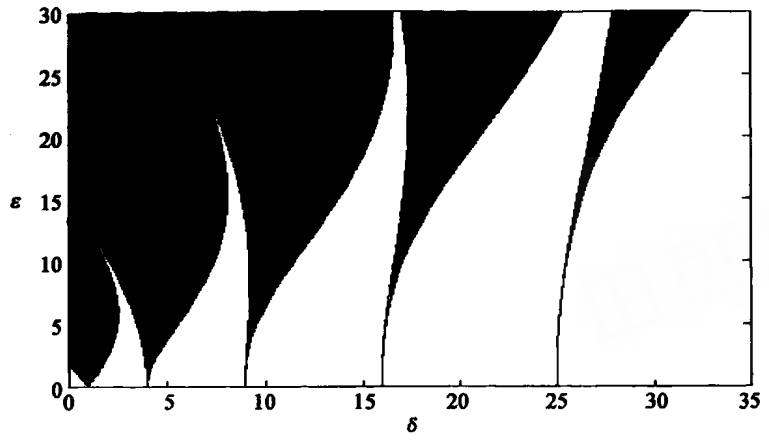

(a) M=0

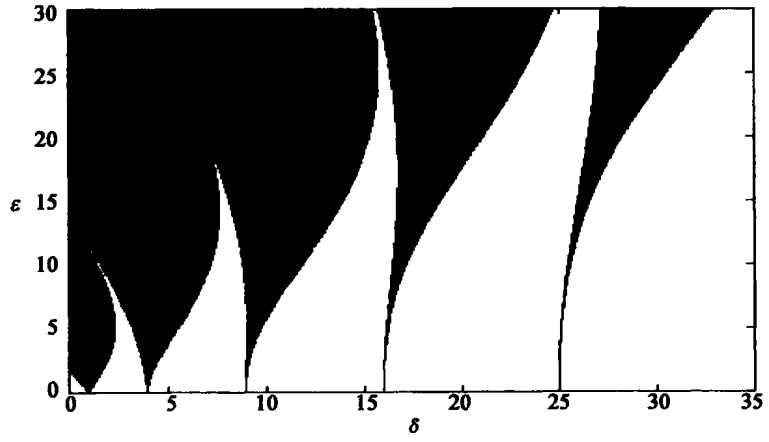

(b) M=0.1085

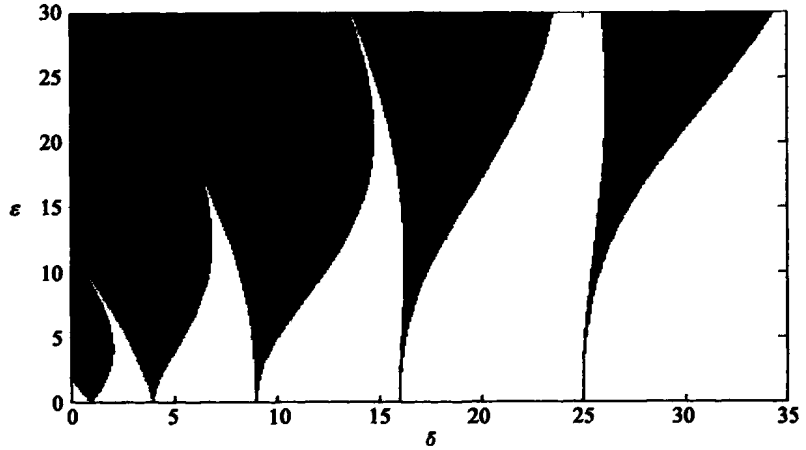

(c) M=0.3014

Fig. 3. Hill instability charted up to large parameters (shade regions are unstable).

According to Fig. 3, it seems that higher-order regions of instability are more sensitive to M than lower-order ones. Increasing M value, the first and second instability regions become a little narrower. And the third, fourth and fifth instability regions become broader. All the instability regions are displaced towards the left of the figure. Fig. 3(a) shows the instability chart of Hill equation (24) when $M = 0$, which is also called the Mathieu instability chart or the Ince-Strutt chart. It is clear that the instability of a tether is not only related to the platform heave motion, but also might be caused by the platform surge motion.

4. Case Studies

Some case studies are carried out to analyze the dynamic response characteristics in different instability regions. The tether is excited by the combined platform surge and heave motion, and it is modeled as a linear beam and a nonlinear beam respectively. Input data for case studies are listed in Table 1, which is the same as the reference presented by Patel and Park (1995). The ratio of time-varying axial force amplitude to pretension N^*/N_0 is set to be 1.0, according to which the platform heave motion amplitude can be obtained. Two different M values of 0 and 0.1085 are chosen for case studies. The relation between instability region number and excited periods is shown in Table 2. Firstly, the results obtained by linear and nonlinear model are compared with each other in the un-damped case. Then the effect of damping is investigated. Only the leading four modes are adopted for the transverse nonlinear vibration analysis of the tether, because the leading four modes can not only simplify the computation but are also an adequate approximation.

Table 2 Relation of instability region number and excited periods

Excited period (s)	Linear beam model		Nonlinear beam model	
	δ^*	Instability region	δ	Instability region
8.5	8.3	Third stability	9.2	Mid third
11.4	15	Fourth stability	16.6	Mid fourth
15.3	27	Fifth stability	29.9	Mid fifth

Fig. 4 shows the response magnitudes at mid-point of the tether. The corresponding results have been obtained with $C_D = 0$. Assuming the period of platform motion is limited in the range of 6 ~ 30 seconds, so we did not calculate the dynamics response in the first and the second instability regions herein. A comparison is made between the results obtained by nonlinear beam model and those obtained by linear one, which is the same as Patel's model (Patel and Park, 1995). It can be seen that the dynamic response results are unstable in the instability regions by use of nonlinear model, while the results obtained by Patel's model (Patel and Park, 1995) are stable. The reason is that, if the coupled axial and transverse vibrations of the tether are considered, the instability regions of Hill equation (16) and the Mathieu equation (22) are different. It can be clearly observed in Table 2 and Fig. 3, indicating that the interaction between axial and transverse is significant.

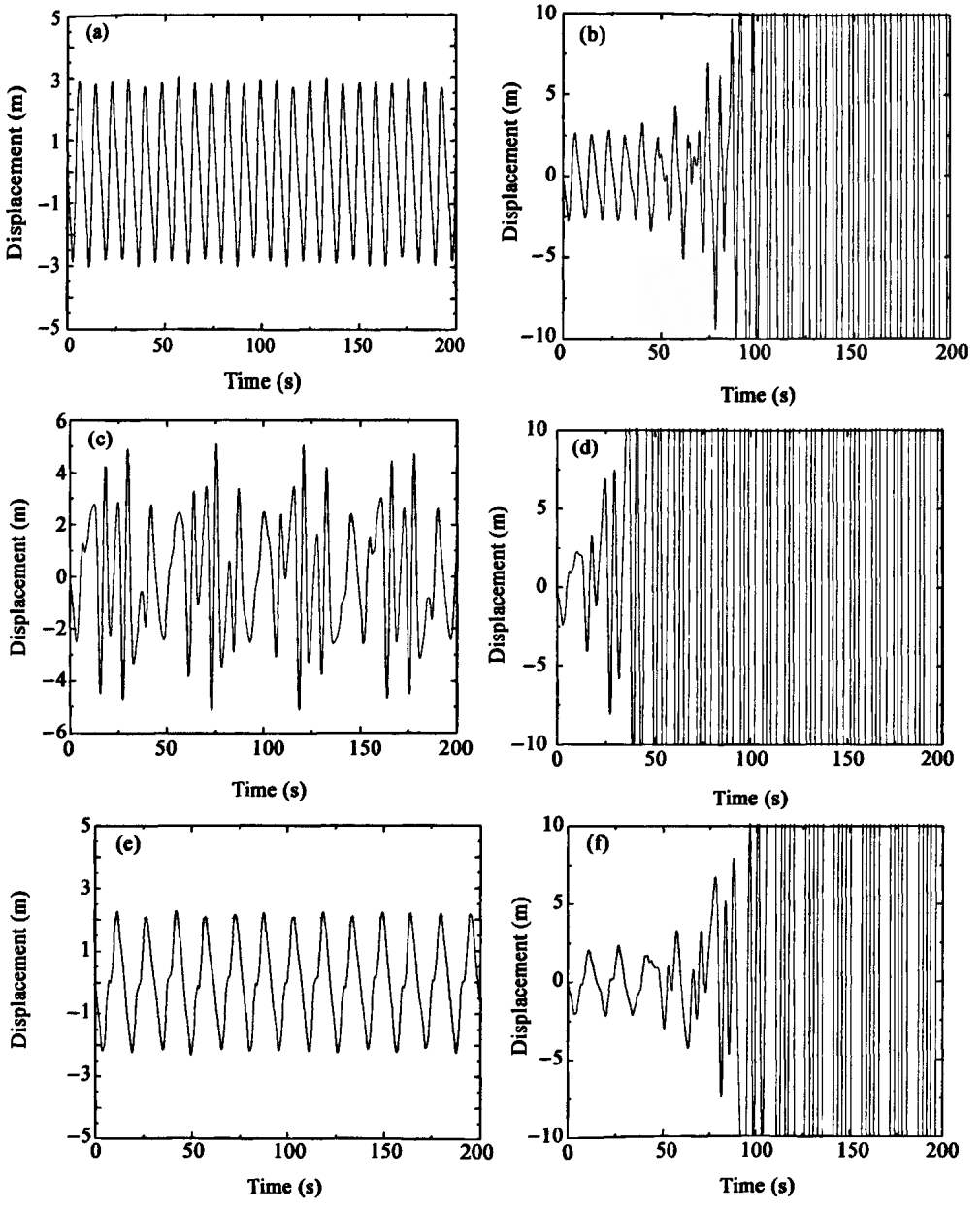

Fig. 4. The response magnitudes at the mid-point of the tether in different instability regions, without damping. (a) $M=0$, $\delta^*=8.3$, (b) $M=0.1085$, $\delta=9.2$, (c) $M=0$, $\delta^*=15$, (d) $M=0.1085$, $\delta=16.6$, (e) $M=0$, $\delta^*=27$, (f) $M=0.1085$, $\delta=29.9$.

While constructing the Hill instability chart and calculating the tether dynamic response in different instability regions, the damping term is not considered. In reality, the nonlinear hydrodynamic damping plays an important role in limiting tether oscillations. This feature is studied below. Fig. 5

plots the response magnitudes at the mid-point of the tether including the effect of damping. It is noted that even if a tether is in an unstable condition, the response will be stable and the amplitude will be limited.

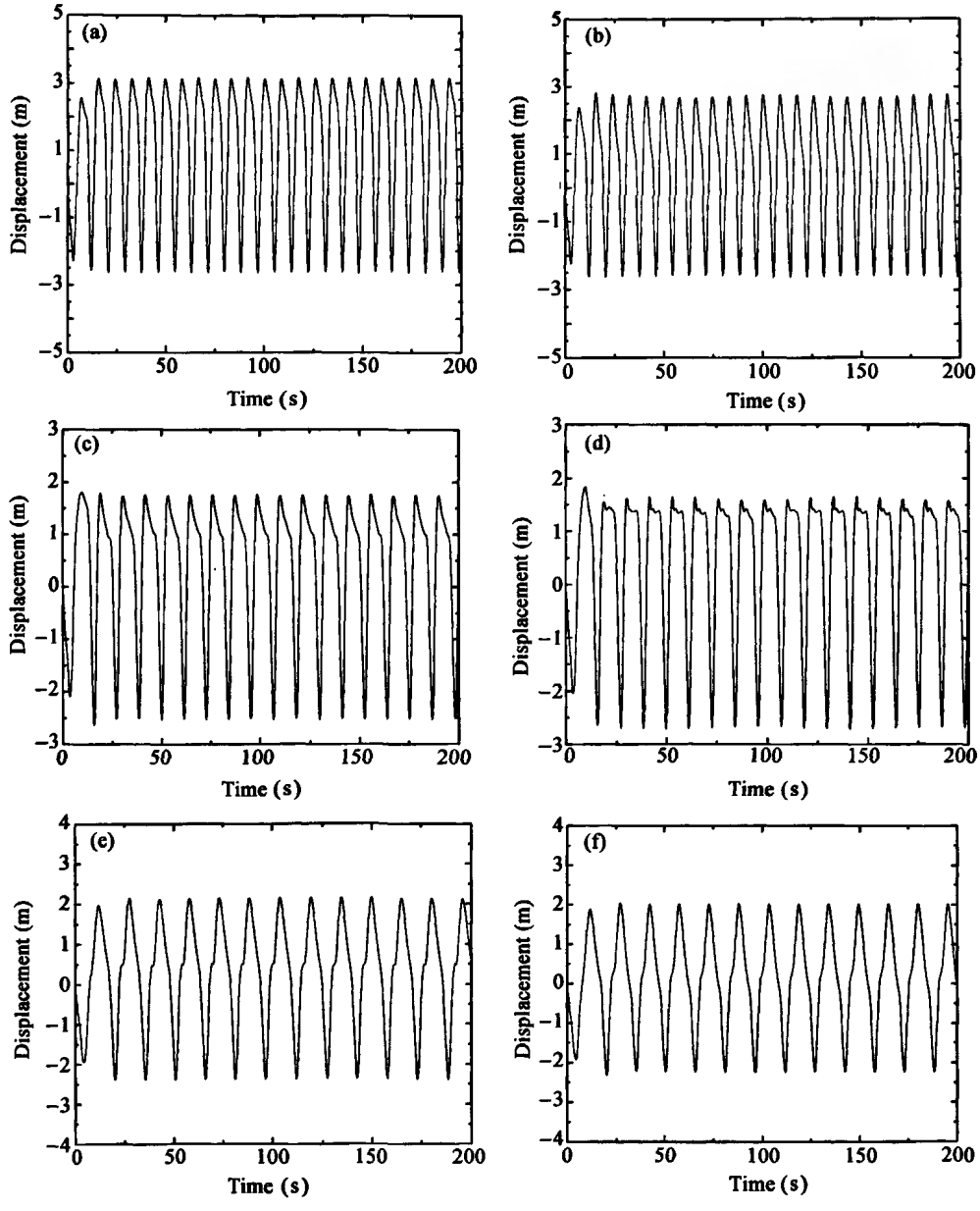

Fig. 5. The response magnitudes at the mid-point of the tether in different instability regions, with damping. (a) $M=0$, $\delta^*=8.3$, (b) $M=0.1085$, $\delta=9.2$, (c) $M=0$, $\delta^*=15$, (d) $M=0.1085$, $\delta=16.6$, (e) $M=0$, $\delta^*=27$, (f) $M=0.1085$, $\delta=29.9$.

The above results show that the dynamic response predicted by nonlinear model is different from that of linear beam model, and it is more realistic than linear beam model for accurate dynamic analysis of TLP tether subjected to the combined platform surge and heave motions.

5. Conclusions

The analysis presented in this paper demonstrate the significant effects of the nonlinear coupling between the axial and transverse vibrations of TLP tether. It is not frequently considered in conventional design studies, if the nonlinear beam model is used. The governing equation of the tether is not Mathieu equation anymore, it becomes Hill equation. The Hill stability charted up to large parameters is obtained by the Hill's infinite determinant and harmonic balance method, which is definitely different from Ince-Strutt chart when M has a large value. The Hill instability chart prescribed in this paper should be used to guide the design work of TLP tether. The case studies prove the significance of considering nonlinear coupling once more.

However, some assumptions are made for the simplification in above investigation, thus further work needs to be carried out to ignore these assumptions, such as the consideration of coupling between platform and tether dynamics. The study is not limited only in 2D space anymore.

References

Chandrasekaran, S., Chandak, N. R. and Anupam G., 2006., Stability analysis of TLP tethers, *Ocean Eng.*, **33**(3-4): 471 ~ 482.

Chatjigeorgiou, I. K., 2004. On the parametric excitation of vertical elastic slender structures and the effect of damping in marine applications, *Appl. Ocean Res.*, **26**(1-2): 23 ~ 33.

Chatjigeorgiou, I. K. and Mavrakos, S. A., 2002. Bound and unbounded transverse response of parametrically excited vertical marine risers and tensioned cable legs for marine applications, *Appl. Ocean Res.*, **24**(6): 341 ~ 354.

Chatjigeorgiou, I. K. and Mavrakos, S. A., 2005. Nonlinear resonances of parametrically excited risers- numerical and analytic investigation for $\Omega = 2\omega_1$, *Comput. Struct.*, **83**(8-9): 560 ~ 573.

Han, S. M. and Benaroya, H., 2000a. Nonlinear coupled transverse and axial vibration of a compliant structure 1: formulation and free vibration, *J. Sound Vib.*, **237**(5): 837 ~ 873.

Han, S. M. and Benaroya, H., 2000b. Nonlinear coupled transverse and axial vibration of a compliant structure 2: forced vibration, *J. Sound Vib.*, **237**(5): 874 ~ 899.

Hsu, C. S., 1975. The response of a parametrically excited hanging string in fluid, *J. Sound Vib.*, **39**(3): 305 ~ 316.

Jefferys, E. R. and Patel, M. H., 1982. On the dynamics of taut mooring systems, *Eng. Struct.*, **4**(1): 37 ~ 43.

Koo Bon-Jun, 2003. *Evaluation of the effect of contact between risers and guide frames on offshore spar platform motions*, Ph.D. thesis, Texas A&M University.

Kuiper, G. L., Brugmans, J. and Metrikine, A. V., 2007. Destabilization of deep-water risers by a heaving platform, *J. Sound Vib.*, **310**(3): 541 ~ 557.

Park, H. I. and Jung, D-H, 2002. A finite element method for dynamic analysis of long slender marine structures under combined parametric and forcing excitations, *Ocean Eng.*, **29**(11): 1313 ~ 1325.

Patel, M. H. and Park, H. I., 1991. Dynamics of tension leg platform tethers at low tension-part 1: Mathieu stability at large parameters, *Mar. Struct.*, **4**(3): 257 ~ 273.

Patel, M. H. and Witz, J. A., 1991. *Compliant Offshore Structures*, Butterworth Heinemann, Oxford.

Patel, M. H. and Park, H. I., 1995. Combined axial and lateral responses of tensioned buoyant platform tethers,

Eng. Struct., **17**(10): 687 ~ 695.

Patel, M. H. and Seyed, F. B., 1995. Review of flexible riser modeling and analysis techniques, *Eng. Struct.*, **17** (4): 293 ~ 304.

Simakhina, S. V., 2003. Stability Analysis of Hill's equation, Chicago.

Thampi, S. K. and Niedzwecki, J. M., 1992. Parametric and external excitation of marine risers, *J. Eng. Mech.*, **118**(5): 943 ~ 960.

WANG Tao and ZOU Jun, 2006. Hydrodynamics in Deepwater TLP tendon design, *Journal of Hydrodynamics (Ser. B, Supplement 1)-Proceedings of the Conference of Global Chinese Scholars on Hydrodynamics*, Shanghai, China, 11-14 July 2006, **18**(3): 386 ~ 393.

Yigit, A. S. and Christoforou, A. P., 1996. Coupled axial and transverse vibrations of oilwell drillstrings, *J. Sound Vib.*, **195**(4): 617 ~ 627.

Zhang, L. B., Zou, J. and Huang, E. W., 2002. Mathieu Instability Evaluation for DDCV/Spar and TLP Tendon Design, *Proc of the 11th Offshore Symposium*, *SNAME*, Houston, TX.